

VIRTUAL WIND TUNNEL: AN EFFICIENT COMPUTATIONAL TOOL FOR AEROELASTIC ANALYSIS AND DESIGN OF INFLATABLE STRUCTURES

JOSE M. GONZALEZ^{*}, ENRIQUE ORTEGA^{†,*}, JORDI PONS-PRATS^{ξ,*}, MERCÈ LOPEZ^{*}, ROBERTO FLORES^{*}, JAVIER MARCIPAR^ψ, EUGENIO OÑATE^{*}

^{*} International Center for Numerical Methods in Engineering (CIMNE)
Universidad Politécnica de Cataluña
Campus Nord, Edifici C1, 08034 Barcelona, Spain - Web page: <http://www.cimne.com>
josem.gonzalez@cimne.upc.edu
onate@cimne.upc.edu
rflores@cimne.upc.edu
mlnunez@cimne.upc.edu

[†] Escola Superior d'Enginyeries Industrials, Aeroespacial i Audiovisual de Terrassa (ESEIAAT)
Universidad Politécnica de Cataluña
Rambla Sant Nebridi 22, Edifici Gaia, 08222 Terrassa, Spain
e.ortega@upc.edu

^ξ Escola d'Enginyeries de Telecomunicacions i Aeroespacial de Castelldefels (EETAC)
Esteve Terrades 5, Campus PMT-UPC C, Edifici C3, 08860 Castelldefels, Spain
jpons@cimne.upc.edu

^ψ Buildair – Engineering & Architecture S.A.
Horta st. 6, Warehouse 3,4,5. Pol. Ind. El Pla. 08750, Molins de Rei - Barcelona - Spain
marcipar@buildair.com - Web page: <http://www.buildair.com>

Key words: Inflatable structures, fluid-structure interaction, panel methods, detached-flow corrections.

Summary. This paper presents the Buildair Virtual Wind Tunnel, a new computational tool developed for the aeroelastic analysis and design of inflatable structures. The work describes the numerical methodology proposed to solve the fluid-structure interaction problem and the graphical user interface, designed specifically for inflatable hangars. Finally, a practical application involving a Buildair H20 hangar under wind loads is presented. The results are discussed and compared to those obtained with current analysis methods at the company. The work highlights the advantages of the proposed methodology and the importance of including aeroelastic effects in the design and analysis of inflatable hangar structures.

1 INTRODUCTION

Inflatable structures is an innovative field in civil engineering that poses important challenges from the point of view of analysis and design^{[1],[5]}. Conventional approaches based

on building standards help estimate wind or snow loads, but being typically intended for rigid structures, they do not account for aeroelastic and dynamic effects. The results obtained generally lead to conservative solutions that, although useful in the early design stages, are not accurate enough to carry out detailed analyses and structural optimization. In addition, the characteristics of the materials and the shapes employed in inflatables can go beyond those observed in the standards, adding an additional layer of complexity to the problem.

Alternative approaches based on Fluid-Structure Interaction (FSI) methods with different degrees of fidelity can also be employed for detailed analyses. However, the computational cost involved generally makes these prohibitive in the context of practical design, where time and computer resources are limited and multiple studies are often required to assess sensitivities. Hence, methods that yield acceptable accuracy while minimizing the solution cost are necessary.

With this objective, CIMNE has made significant efforts^[7] to develop a methodology that allows practical analyses of parachutes and deformable structural membranes with a manageable computational cost. The computer program Buildair Virtual Wind Tunnel (VWT) involves most of these developments and is specifically intended for inflatable hangars. The tool enables realistic FSI simulations with affordable computational cost. The solution approach combines potential flow aerodynamics, explicit FE structural dynamics and staggered FSI coupling. The aerodynamic solver is a low-order panel method with empirical corrections to account for flow separation effects. The detached flow areas are automatically predicted using Stratford's method and the pressure in the wake region is adjusted with an ad-hoc empirical model. On the structural side, the solver uses a large-displacement Finite Element discretization that models cable, membranes and 3D solids. In the VWT special attention has been given to the graphical user interface. It is based on CIMNE's pre and post-processing system GiD^[4], and is designed for ease of use and to minimize the time required for the problem setup, solution and analysis of results. The post-process tools offer advanced solution analysis and visualization capabilities, including modules for dynamic results through filtering and statistical treatment. The most salient features of the methodology and application results are described in this work.

The paper is organized as follows. The numerical model proposed for solving the FSI problem is described in Section 2. The computational tool and its graphical interface are presented in Section 3 and several numerical results and comparison with other methods used in the company are presented in Section 4. Finally, important aspects of the methodology and future lines of investigation are highlighted in Section 5.

2 NUMERICAL MODEL

The numerical methodology is designed to meet practical requirements in the analysis of inflatable hangars. As mentioned in the introduction, the objective is to enable realistic fully coupled simulations with affordable computational cost and hardware resources. An overview of the FSI solution approach is presented below and details can be found in^{[8],[9]}.

2.1. Structural model

The structural solution is based on a large displacement – small strain FE formulation, which includes a wrinkling model to allow buckling of selected materials when subjected to compressive loads. The solver models cables, membranes and 3D solids using 2-node linear, 3-node triangular and 4-node tetrahedral elements, respectively. The line elements are used for the hangar anchorage and stabilization cables, also for straps and reinforcement tapes. The fabric is modeled with triangle elements. The solid tetrahedral elements can be used to model ballasts and any other suitable components.

Once discretized, the resulting semi-discrete equations are advanced in time using a second-order explicit scheme. Although conditionally stable, this scheme allows to solve highly nonlinear problems with robustness and efficiency. A numerical dissipation model with Rayleigh damping and bulk viscosity is also used to control local high-frequency modes.

The solver allows applying to the model different types of kinematic constraints and analytical contact with pre-defined surfaces. Time-varying tube pressurization (for inflation and deflation analyses) and distributed loads (e.g. fixed-direction and follower) to simulate wind and snow actions also can be prescribed.

2.2. Aerodynamic model

The flow around the hangar is solved with a low-order unsteady panel method with doublets and sources (see^{[8],[2],[3]} for details). In addition to being faster and efficient, this approach has the advantage that it only needs the external faces of the structural mesh for calculation (no fluid volume mesh is required). This largely reduces the computational cost and facilitates the solution of flows around deformable bodies as well as the implementation of the coupled scheme. The aerodynamic solver includes empirical models for simulation of added mass effects and drag forces on cables and simple bodies. In addition, exponential wind profiles according to the Eurocode 1 standards (EN 1991-1-4: wind actions)^[1] can be used to model the effects of atmospheric boundary layers.

This methodology is simple and effective, but only suitable for streamlined bodies where the flow remains mostly attached. This is not the case in a hangar, where extensive flow separation occurs as the result of its blunt shape. Therefore, a correction of the calculated pressure loads has also been proposed to include the effects of flow separation.

The pressure correction is based on the particular characteristics of high Reynolds flows around blunt bodies. In such cases, experiments show that the velocity and pressure fields on areas where the flow remains attached do not differ much from an inviscid solution. However, when detachment occurs, the time-average pressure and velocity in the near-wake becomes almost constant. Following these observations, the idea in this work is to use the inviscid solution (which is considered realistic until detachment) to automatically determine the separated flow areas and keep the downstream pressure constant. The correction procedure consists of the following four main steps:

1. Detection of the stagnation flow areas and calculation of the flow streamlines from the inviscid velocity field.

2. Estimation of the flow separation point along each streamline using the inviscid solution and Stratford's criterion^[11].
3. Empirical correction of the calculated pressure downstream detachment points.
4. Smoothing of the pressure field in the detached flow area.

The proposed separation method allows modeling fully turbulent flow (A suitable choice in most cases), but laminar-turbulent transition can also be taken into account. Michel's method^[6] is used to determine the location of the transition points along the flow streamlines.

2.3. Coupling scheme

The structural and aerodynamic solvers are coupled using a 2-way staggered scheme, with one fluid solve and one structure solve per time step. Since the mesh is the same, no interpolation of results is required during the simulation. This allows obtaining both the transient and steady-state response of the structure in a very efficient way. It should be noted that in typical calculations the time step increment of the structural solver is small due to the explicit approach, thus, several structural time increments are performed per aerodynamic step. Although this could affect the high-frequency response, it is not a serious limitation because these modes usually have low amplitude, and affect only small parts of the structure. On the contrary, the low frequency modes, which govern the overall response of the structure, can be well resolved. Added mass effects can also be accounted for in the simulation, and the introduction of additional artificial damping (see^[2]) allows control the stability of the simple coupling strategy adopted.

3 THE BUILDAIR VIRTUAL WIND TUNNEL

The Buildair VWT is a computational tool developed on the basis of the CIMNE's pre- and post-processor system GiD^[4]. Since the VWT is especially designed for the simulation of inflatable hangars, most of the required processes on geometry and the definition of the simulation parameters have been automated to minimize the manual work required. In a typical simulation, the graphical interface guides the user through a set of sequential windows, organized into pre and post-process stages, where the relevant data is defined. The pre-process involves all the tasks required for generation/import and preparation of the CAD model, definition of materials and boundary conditions and mesh discretization. After the problem setup is complete, the calculation engine runs the simulation. Once finished, the post-process stage offers different tools for visualization and analysis of the results as well as automatic report for specific studies. The main steps in a typical simulation are described in the next.

3.1. Pre-process stage

The pre-process involve six main steps, each with its corresponding windows menu as shown in Figure 1. The workflow requires definition of:

1. Model and type of analysis: import or automatic generation of the model; type of analysis: snow (structural run), wind (FSI) or inflation (FSI or structural only).
2. Wind conditions: speed, direction, boundary layer profile and air properties.
3. Aerodynamic conditions and simulation parameters.

4. Boundary conditions (kinematic constraints and loads).
5. Material properties (pre-loaded database for typical textile membranes, straps and cables).
6. Simulation and meshing parameters.

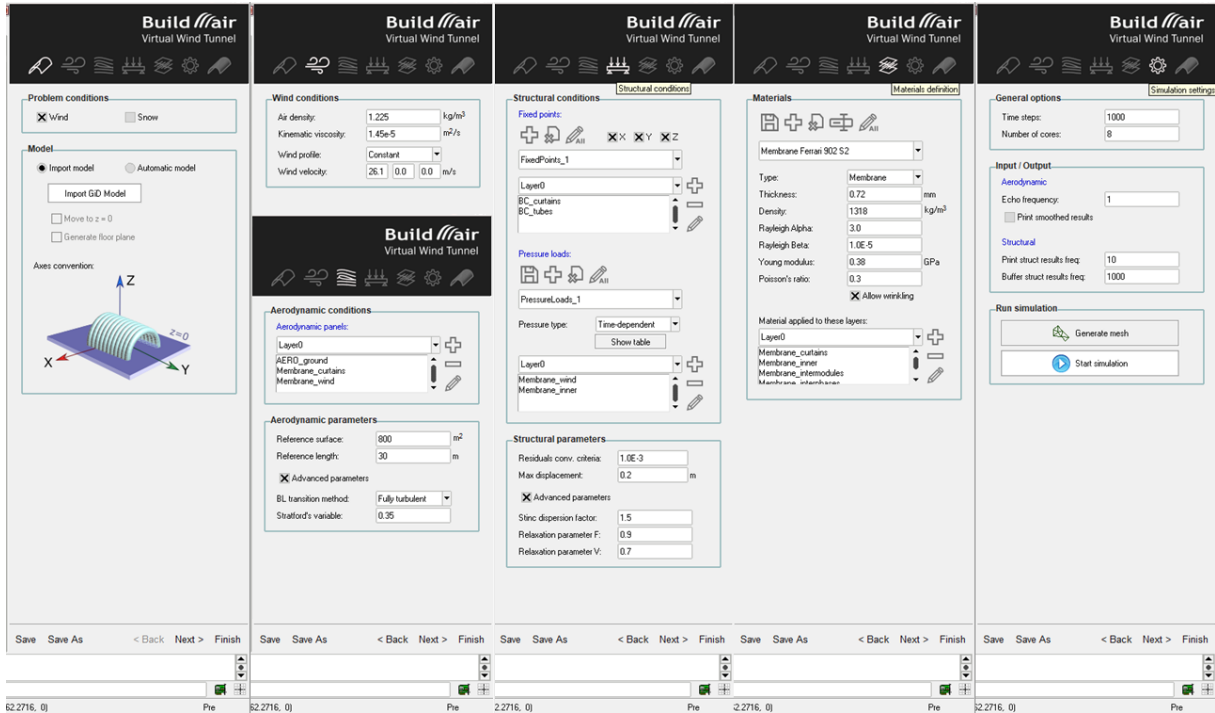


Figure 1: Buildair VWT, pre-process windows. From left to right: a) type of problem b) wind & aerodynamic conditions c) boundary & load conditions d) materials e) meshing

It is important to note that the pre-process stage also provides the user with cost estimates (materials, manufacturing, etc.) useful for marketing and decision making analyses.

3.2. Post-process

The post-process options are displayed in a single dialog box where the user can choose different options for visualization and analysis (see a view in Figure 2). Among them:

1. Time deformation of the structure.
2. Contour graphs of the calculated results (organized according to categories).
3. Time series for the calculated results and relevant data for dynamic analysis.
4. Max-Min and design values for instant or averaged data.
5. Animation of the results and video generation.
6. Automatic reports with the relevant simulation parameters and results.

The post-process also includes additional capabilities such as export of the model in DXF format (for technical report purposes), frequency analyses of select dynamic data and the generation of a database for structural optimization purposes.

It is worth mentioning that the computational tool described above has been tailored according to the specific requirements and analysis procedures at Buildair. Nonetheless, the VWT can easily be customized to meet other particular requirements.

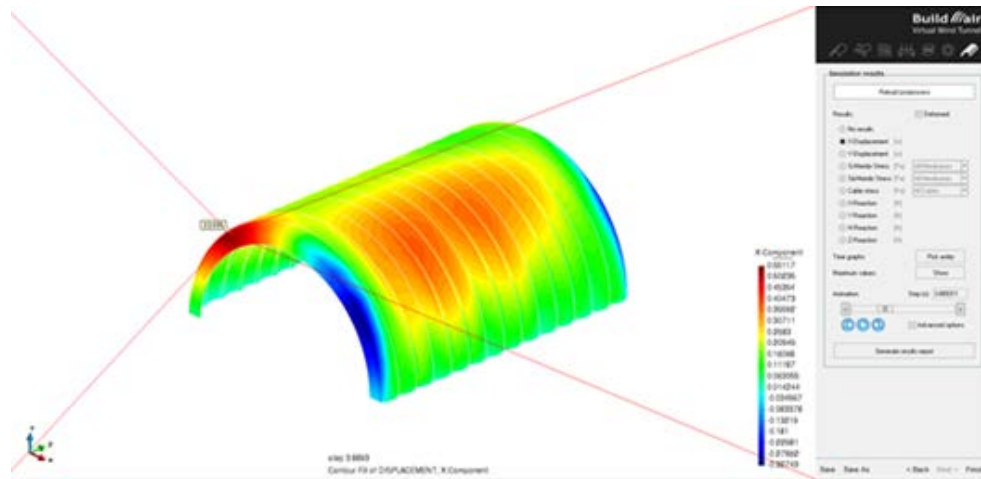


Figure 2: Buildair VWT, post-process example: contour plot of transversal displacements with location of maximum value.

4 APPLICATION EXAMPLE

In order to assess the performance of the VWT, this section presents a realistic test case based on a Buildair H20 hangar. The suitability of the solution is evaluated by comparison with results obtained from building standards (EC-1991-1-4) and calculated with the software RAMSeries^[10], developed by the company Compass and commonly used in Buildair.

4.1. Computational model and problem setup

The H20 is a medium-size inflatable hangar designed and manufactured by Buildair. It has free width and height of 20 and 11 m, respectively, and consist of 11 tubes of 2.84 m in diameter each. The total length of the hangar is 31.2 m and the nominal inflation pressure of the tubes is 2000 Pa (20 mbar).

The H20 is built of groups of structural elements composed by textile membranes, polyester straps and steel plate anchorages. Both the structural function and resulting loads on the materials are different, namely:

- Textile membranes conform the inflated tubes and the curtains. Although the membrane in contact with adjacent tubes behaves a little different from the rest of the tube because of the anchorage, in general, only axial plain stresses are considered for design purposes.
- Polyester straps conform a net surrounding the inflated tubes that aims to increase the stiffness and stability of the structure and transmit the forces to the anchorages. Typically, the straps are 0.3 m wide and are located along longitudinal (*spines*, maximum generatrix, *ribs*, close to interphase between tubes) and circumferential tube directions (*braces*).
- Anchorages: they consist of steel plates where the straps are tied and sewn (along the

main body of the hangar). Eyebolts are used along the curtains.

In this study, frontal and lateral wind conditions (i.e. along longitudinal and transversal directions) are simulated. An atmospheric wind profile according to Eurocode standards^[1] is defined with basic speed of 25 m/s. The analysis geometry includes a ground (symmetry) plane and the resultant mesh consists of 31k quadrilateral elements and 22k nodes. Some views of the model are presented in Figure 3.

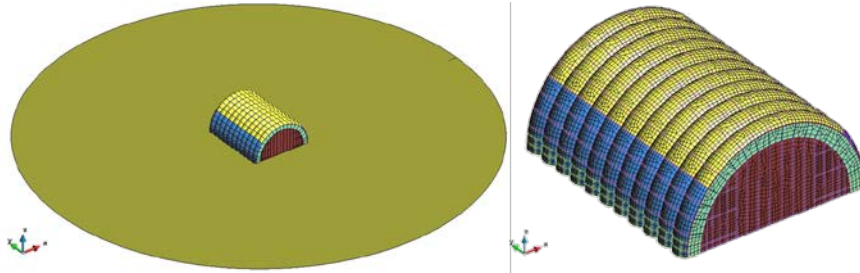


Figure 3: H20 numerical model. Left: geometry with ground reference. Right: hangar discretization

4.2. Numerical results

The numerical results analyzed here are typical at a design stage. These involve pressure distributions, hangar deformations, membrane stresses, forces along the straps and forces on the anchorages.

4.3. Pressure distribution

The pressure distribution on the hangar is studied first for lateral wind. The results presented in Figure 4 compare the pressure coefficient calculated with the VWT (coupled solution) along different transversal sections against reference values from the building standard. It is possible to observe that the calculated pressure distribution reasonably agrees with the standard, but the VWT total load is less conservative. This should be expected because the standard considers a simple pressure distribution with a few contributory areas, and also lacks of aeroelastic effects.

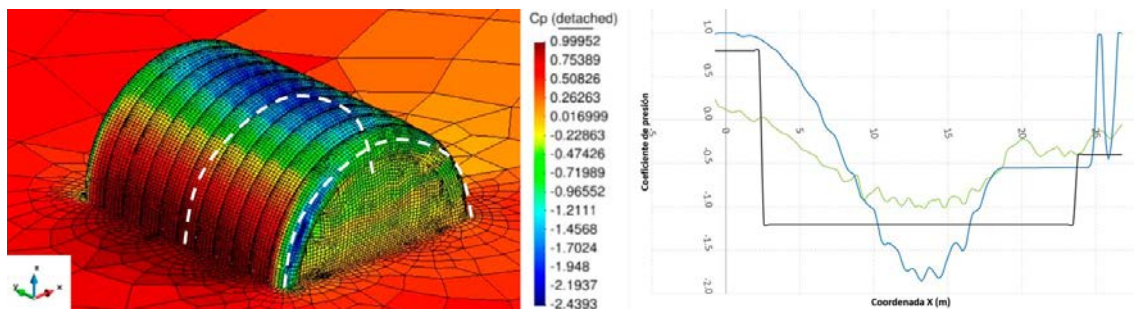


Figure 4: Calculated pressure coefficient under transversal wind (left) and comparison with the building standard EC-1991-1-4 along selected sections (right).

Hence, in order to check the suitability of the VWT solution, and additional comparison with

quasi-steady CFD results (calculated on a previously deformed hangar) is shown in Figure 5. The results show good agreement and satisfactory prediction of the flow detachment point. Despite a slightly higher suction load at the roof (because of the inviscid approach), the predicted section load compares well with the CFD result. This demonstrates that the VWT can provide realistic design loads but at a fraction of the cost of higher-fidelity simulations.

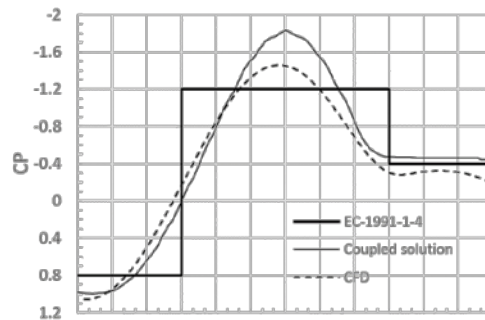


Figure 5: Comparison of pressure distributions along the central tube for transversal wind conditions.

The calculated pressure distribution is also studied for longitudinal wind in Figure 6. It is possible to observe that the VWT delays the detachment around the windward tube and consequently the resultant pressure is lower. Downstream, the hangar surface is not smooth and this has an effect on the inviscid solution and also on the prediction of flow detachment. This probably leads to lower loads, but not far from those obtained from the standard.

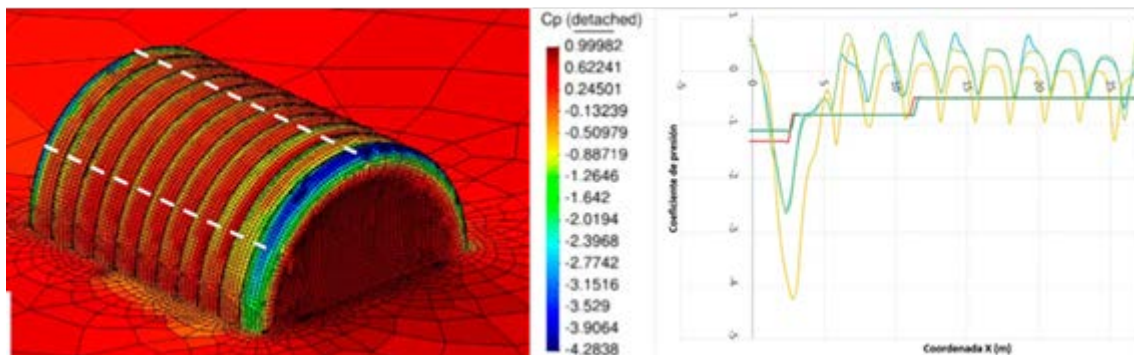


Figure 6: Calculated pressure coefficient under longitudinal wind (left) and comparison with the building standard EC-1991-1-4 along selected sections (right).

4.4. Deformation

The deformation of the hangar caused by wind loads can change the interior working space and its study is very important to guarantee the operation conditions. A critical situation can arise due to the displacement of the curtains under frontal wind. Figure 7 shows a comparison of the deformation in the longitudinal direction calculated with the VWT to that resulting from applying the design values from the building standard. The maximum deformation are significantly lower in the VWT simulation (1.56 m) with respect to the standard (3.11m). As seen before, by design building regulations leads to conservative values. According to the

experience of the company, the lower deformations predicted by the VWT are closer to the behavior observed in practice. Here, the effects of deformation on the resultant pressure field plays an important role. A comparable behavior is observed in Figure 8 for the deformations under lateral wind (0.27 and 0.62m for the VWT and building regulations, respectively). It is also important to note that maximum deformation occurs at different locations, this could be result of the simplified model used by the standard, where only a few contributory constant pressure areas are defined along the hangar.

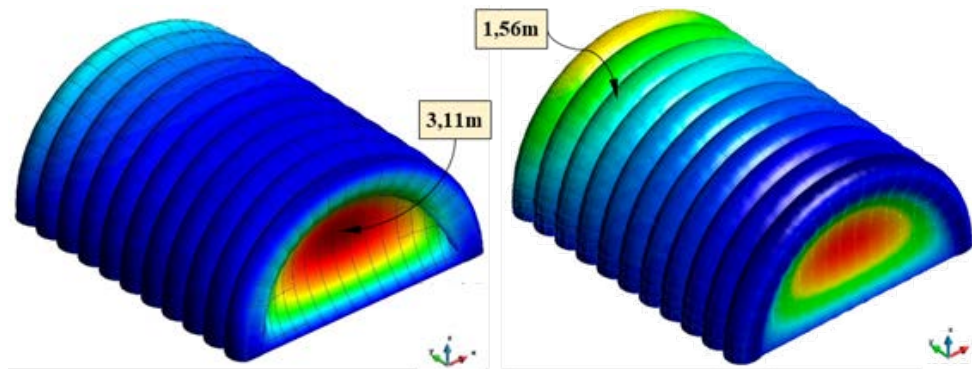


Figure 7: Longitudinal deformation under frontal wind. Left: loads from EC-1991-1-4. Right: VWT coupled simulation.

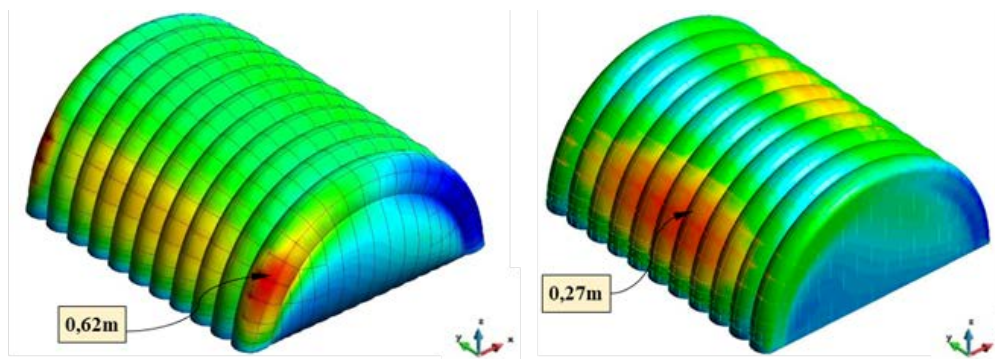


Figure 8: Transversal deformation under lateral wind. Left: loads from EC-1991-1-4. Right: VWT coupled simulation.

4.5. Internal forces

The internal forces acting on the membranes and straps are of the most concern for proper structural design and safe of operation. In the case of the textile membranes, the relevant design values are located at the interphases of the tubes and in the curtains, which are usually analyzed separately. Figure 9 shows the membrane forces under lateral wind. The location of the maximum values is the same for both calculation methods, but the resulting magnitudes are lower in the VWT (15 and 4.7 kN/m) than those from the building regulations (38 and 15 kN/m). The analysis under frontal wind shows similar trends, with lower internal forces over the membranes.

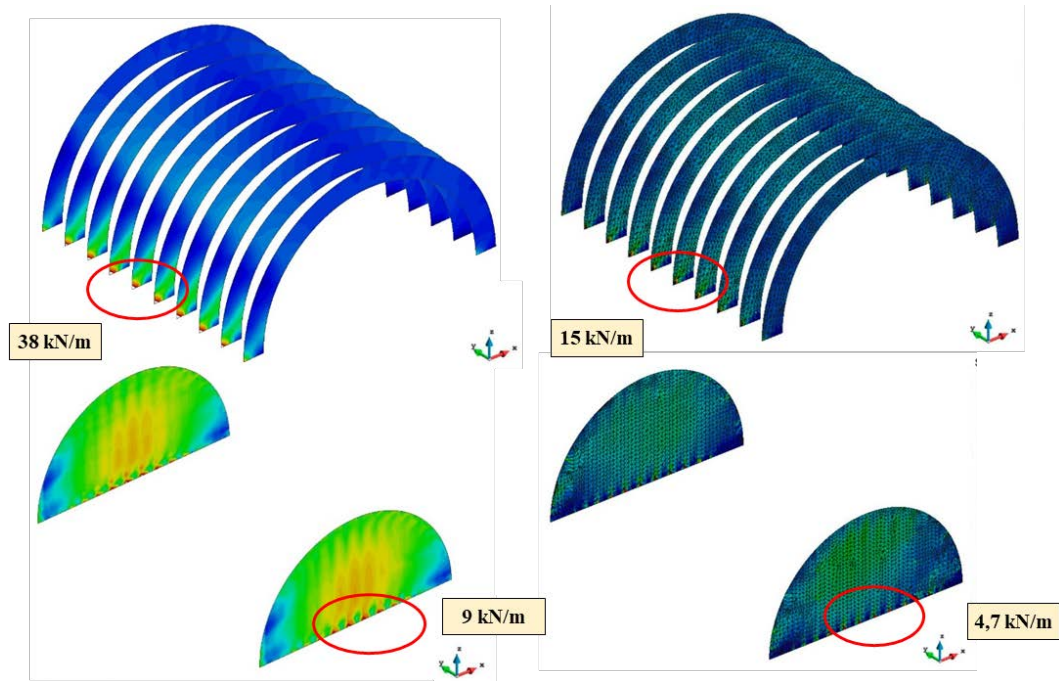


Figure 9: Membrane stresses on tube interfaces (upper) and curtains (bottom). Left: results with loads from EC-1991-1-4. Right: VWT coupled simulation.

The analysis of the straps shows similar trends regarding frontal and lateral winds, but the VWT predicts higher stresses for the spines, ribs and braces (max. value 47,3 kN) than the method using the standard loads (max. value 25,1 kN), see Figure 10.

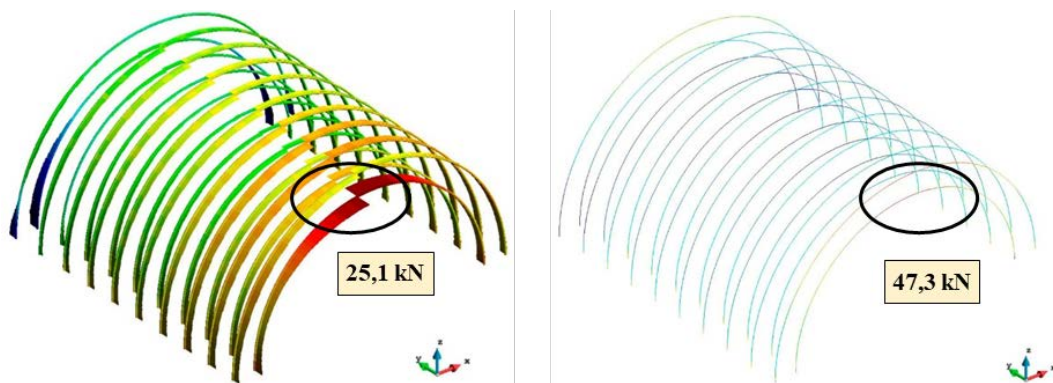


Figure 10: Strap forces. Left: results with loads from EC-1991-1-4. Right: VWT coupled simulation.

These results lead to the conclusion that the VWT implementation reduce the load of the membranes while straps assume this increment of internal force. To some extent, this can be explained by the differences in the loads distributions, but further investigation is required.

4.6. Anchorage forces

Estimation of the forces (reactions) on the anchorages are very important at design stage because of their direct relation to the safety of operation of the hangar. The results obtained for lateral wind are displayed in Figure 11. The VWT gives lower resultant forces (max. value 26,2 kN) in comparison with those obtained when the standard loads are applied (max. value 12.1 kN). A similar behavior is observed under frontal wind loads.

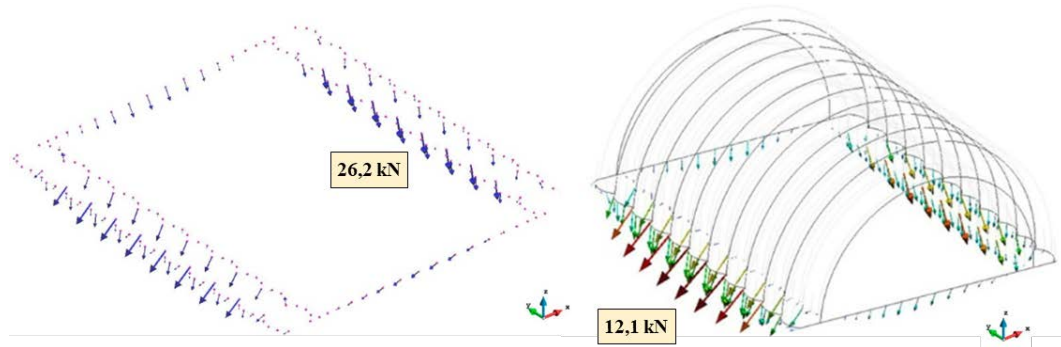


Figure 11: Anchorage forces (modulus). Left: results with loads from EC-1991-1-4. Right: VWT.

Finally, the results obtained for frontal and lateral wind conditions are summarized in Table 1 (lower values are indicated in red). In addition, some relevant aspects of the comparisons are highlighted below.

Table 1: Summary of maximum design values. Conventional method vs Virtual Wind Tunnel

Maximum values	FRONTAL wind		LATERAL wind		Units
	Conventional	VWT	Conventional	VWT	
Deformation wind direction	3.11	1.56	0.62	0.27	m
Axial forces on tubes	12.0	11.6	15.0	11.8	kN/m
Axial forces on interphases	20,0	6.8	38.0	15.0	kN/m
Axial forces on curtains	8.0	8.9	9.0	4.7	kN/m
Axial forces on Spines	17.3	39.7	20.1	55.2	kN
Axial forces on Ribs	25.1	47.3	22.4	60.5	kN
Axial forces on Braces	4.8	9.4	4.8	6.9	kN
Reactions (modulus)	19.1	9.7	26.2	12.1	kN

- ✓ Global loads and deformations are lower when the aeroelastic effects are taking into account. In this sense, the VWT is closer to high-fidelity predictions and observations in practice.
- ✓ The VWT gives lower membranes stresses, even at the tubes interfaces, but there is not a clear trend regarding the curtains.
- ✓ Forces along the straps results higher for the VWT. Possible effects of differences in the distribution of the applied loads should be investigated.
- ✓ Anchorage forces are lower when aeroelastic redistribution of loads is considered.

Regarding computational cost, the quasi-steady solution in this example requires approximately 1 hour on a 4-core processor desktop computer. The cost is quite affordable and allows small companies and developers to include FSI among their regular practice tools.

5 CONCLUSIONS

The Buildair Virtual Wind Tunnel (VWT) has been presented and evaluated in this work. This computational tool, designed for the effective aeroelastic simulation of inflatable hangars, is based on enhanced potential flow aerodynamics and an explicit dynamic finite element solver for the structure with staggered coupling. The software takes into account most of the analysis procedures relevant to hangars and has a user-friendly interface. This provides guided simplified steps to carry out the simulation and automated procedures intended to reduce the manual work required.

The VWT is currently under testing and validation. This paper focuses on an assessment of the software by comparison with other current analysis practices at Buildair. The analyses indicate the suitability of this new calculation tool and highlights the importance of including aeroelastic effects in the design of inflatable structures. The preliminary results are satisfactory and further experimental validation is planned to allow the VWT be considered as a reference tool for the design and analysis of inflatable hangars.

6 REFERENCES

- [1] Cook, N., *Designers' Guide to EN 1991-1-4 Eurocode 1: Actions on structures, general actions part 1-4. Wind actions*. Thomas Telford Publishing, 2007.
- [2] Flores R., Ortega E. and Oñate E. *Simple and efficient numerical tools for the analysis of parachutes*, Engineering Computations, vol. **31**, issue 5, pp. 957-985. (2014)
- [3] Flores R. and Ortega E. *Efficient aeroelastic analysis of wind loads on inflatable hangars*, Proceedings of IASS Annual Symposium 2019-Structural Membranes. Barcelona (Spain), (2019).
- [4] GiD. "The personal pre and postprocessor" version 14.0 (2018) International Center for Numerical Methods in Engineering (CIMNE) (www.gidhome.com)
- [5] Gonzalez J.M, Marcipar J., Estruch C., Cuartero E., Oñate E. *Numerical simulation of an inflated structure for an aircraft hangar* Proceedings of IASS Annual Symposium 2019 –Structural Membranes, Barcelona Spain, (2019).
- [6] Michel, R., *Etude de la Transition sur les Profils d'Aile; Etablissement d'un Critère de Determination de Point de Transition et Calcul de la Trainee de Profile Incompressible*. ONERA Report, 1951. **1**.
- [7] Oñate E., Flores F.G., Marcipar J. *Membrane Structures Formed by Low Pressure Inflatable Tubes*. New Analysis Methods and Recent Constructions". Textile Composites and Inflatable Structures II. Computational Methods in Applied Sciences, vol 8. Springer, Dordrecht. (2008)
- [8] Ortega E., Flores R. and Pons-Prats J., *Ram-Air Parachute Simulation with Panel Methods and Staggered Coupling*, Journal of Aircraft, vol. **31**, pp. 807-814. (2017).
- [9] Ortega, E., Flores, R., Cuartero, E., & Oñate, *Efficient aeroelastic analysis of inflatable structures using enhanced potential flow aerodynamics*. J. of Fluids and Structures, **90**, 230-245 (2019).
- [10] "RAMSeries Reference manual", "RAMSeries Theory manual" Compass Ingeniería y Sistemas (www.compassis.com)
- [11] Stratford, B.S. *The prediction of separation of the turbulent boundary layer*. Journal of fluid mechanics. Journal of Fluid Mechanics, 1959. 5(1): p. 1-16.